Design, Syntheses and In Vitro Gene Delivery Efficacies of Novel Mono-, Di- and Trilysinated Cationic Lipids: A Structure−Activity Investigation

Priya P. Karmali,† Valluripalli V. Kumar,† and Arabinda Chaudhuri*

Division of Lipid Science and Technology, Indian Institute of Chemical Technology, Hyderabad-500 007, India

Received October 24, 2003

Structure−activity investigation including design, syntheses, and evaluation of relative in vitro gene delivery efficacies of a novel series of cationic amphiphiles (**1**−**10**) containing mono-, di-, and trilysine headgroups are described in CHO, COS-1, and HepG2 cells. Several interesting and rather unexpected transfection profiles were observed. In general, lipid **1** with the myristyl tail used in combination with DOPE as colipid exhibited superior transfection properties compared to (a) the monolysinated analogues with longer hydrocarbon tails (lipids **2**−**4**), (b) the dilysine (lipids **5**−**7**) and the trilysine headgroup analogues (lipids **8**−**10**), and (c) commercially available LipofectAmine with multiple positive charges in its polar region. As a preliminary estimate of the relative DNA-compacting efficacies of these new lysinated cationic lipids, the hydrodynamic diameters of representative lipoplexes were measured using dynamic laser light scattering technique. Our lipoplex size data are consistent with the notion that covalent grafting of an increasing number of positively charged functional groups in the headgroup region of cationic lipids need not necessarily result in more compacted lipoplexes. Both gel retardation and DNase I sensitivity assays indicated similar lipid/DNA binding interactions for all the novel mono-, di-, and trilysinated cationic lipids. MTT-assay-based cell viability results clearly demonstrate that the overall lower transfection properties of trilysine analogues (**8**−**10**) compared to their mono- (**1**-**4**) and dilysinated (**5**−**7**) counterparts are unlikely to originate from differential toxicity related effects. Taken together, the present findings support the notion that caution needs to be exercised in ensuring enhanced gene delivery efficacies of cationic lipids through covalent grafting of multiple lysine functionalities in the headgroup region.

Introduction

Design of efficient cationic lipid based gene delivery reagents as alternatives to potentially immunogenic viral vectors continues to be an intensely pursued area of contemporary research in nonviral gene therapy.[1−17] Cationic transfection lipids (also known as cytofectins) have been amply demonstrated in recent years to be capable of delivering functional genes (lipofection) to murine lungs,[18] rat pulmonary epithelium,[19] and the nasal epithelium of patients with cystic fibrosis.[20] Although details of lipofection pathways are still incompletely understood, the crucial steps include (a) formation of electrostatic complexes (popularly known as "lipoplexes") between polyanionic macromolecular DNA (genes) and the positively charged lipids, (b) endocytotic internalization of the resulting lipoplexes, (c) escape of the DNA from the endosome compartment to the cell cytoplasm, and (d) nuclear trafficking of the endosomally released DNA to access the nuclear transcription apparatus before the final transgene expression in cytosol.[21−24]

Broadly speaking, gene delivery efficacies of cationic lipids depend on their ability to electrostatically compact naked DNA such that the endocytotic cellular uptake of the resulting compacted DNA (lipid/DNA complex) is ensured. Studies aimed at biophysical characterizations of lipoplexes made from cationic lipids with different net cationic charges have been reported.[25] An obvious way of enhancing electrostatic interactions between cationic lipid and DNA is to use cationic lipids with more than one positively charged functional groups in their headgroup regions. This is why the headgroup functionalities of the some of the most widely used commercially available cationic transfection lipids contain more than four positive charges (such as LipofectAmine). However, the transfection efficiencies of a number of monocationic lipids,[26−28] including our own,[1,2,4,6,12,29,30] have been demonstrated to be superior to that of LipofectAmine. Although investigations delineating transfection efficiencies of either purely trilysinated cationic lipids[5,31] or exclusively monolysinated cationic lipids[3,8,32] have been reported, systematic structure−activity investigations using a library of cationic lipids with an increasing number of positively charged headgroups have hardly been undertaken. Toward this end, using a series of novel cationic lipids with mono-, di-, and trilysine headgroups and a common hydrophobic anchor skeleton (lipids **1**−**10**, Schemes 1−3), we demonstrate, for the first time, that the monolysine lipid with a myristyl tail (lipid **1**) exhibits superior transfection efficacies compared to its di- and trilysine analogues in CHO, COS-1, and HepG2 cells. In addition, toward evaluating relative DNA-compacting efficacies of these new lysinated cationic lipids, the hydrodynamic diameters of representative lipoplexes were measured using

* To whom correspondence should be addressed. Phone: 914027193201. Fax: 914027160757. E-mail: arabinda@iict.res.in.

† P.P.K. and V.V.K. contributed equally to this work.

10.1021/jm030541+ CCC: $27.50
Published on Web 02/19/2004

Scheme 1. Synthesis of Lipids **1**−**4** with Monolysine Headgroups[a]

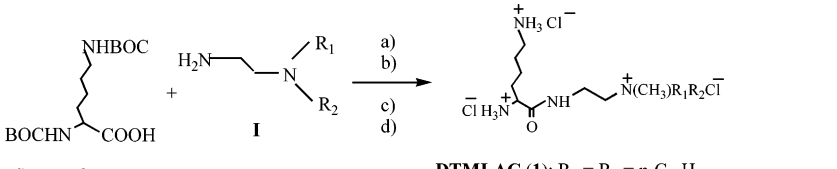

DTMLAC (**1**); $R_1 = R_2 =$ n-$C_{14}H_{29}$
DHMLAC (**2**); $R_1 = R_2 =$ n-$C_{16}H_{33}$
DOMLAC (**3**); $R_1 = R_2 =$ n-$C_{18}H_{37}$
OOMLAC (**4**); $R_1 =$ n-$C_{18}H_{37}$, $R_2 = C_{18}H_{35}$ (oleyl)

[a] Reagents: (a) DCC, HOSu, DMAP; (b) MeI (excess); (c) TFA, DCM; (d) Cl^- ion exchange (AmberlystA-26 resin).

Scheme 2. Synthesis of Lipids **5**−**7** with Dilysine Headgroups[a]

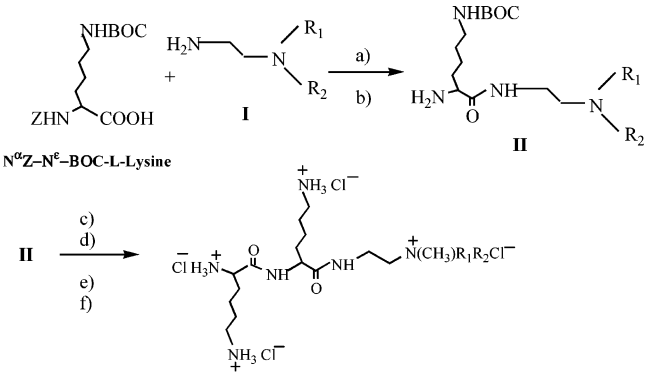

DTML$_2$AC (**5**); $R_1 = R_2 =$ n-$C_{14}H_{29}$
DHML$_2$AC (**6**); $R_1 = R_2 =$ n-$C_{16}H_{33}$
DOML$_2$AC (**7**); $R_1 = R_2 =$ n-$C_{18}H_{37}$

[a] Reagents: (a) DCC, HOSu, DMAP; (b) $HCOONH_4$, 10% Pd/C; (c) BOC(Lys)BOC OH, DCC, HOSu, DMAP; (d) MeI (excess); (e) TFA, DCM; (f) Cl^- ion exchange (Amberlyst resin).

Scheme 3. Synthesis of Lipids **8**−**10** with Trilysine Headgroups[a]

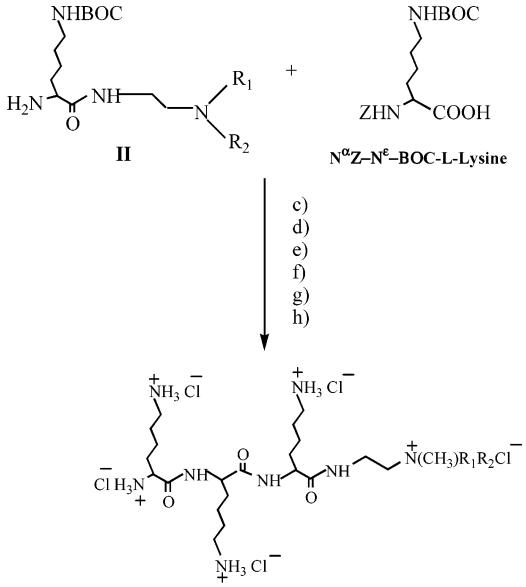

DTML$_3$AC (**8**); $R_1 = R_2 =$ n-$C_{14}H_{29}$
DHML$_3$AC (**9**); $R_1 = R_2 =$ n-$C_{16}H_{33}$
DOML$_3$AC (**10**); $R_1 = R_2 =$ n-$C_{18}H_{37}$

[a] Reagents: (c) DCC, HOSu, DMAP; (d) $HCOONH_4$, 10% Pd/C; (e) BOC(Lys)BOC OH, DCC, HOSu, DMAP; (f) MeI (excess); (g) TFA, DCM; (h) Cl^- ion exchange (Amberlyst resin).

dynamic laser light scattering technique. Taken together, results of the present structure−activity investigation indicate that covalent grafting of multiple positively charged functionalities in the headgroup region need not necessarily impart superior transfection efficacies and enhanced DNA-compacting properties to cationic amphiphiles.

Results and Discussion

Chemistry. Toward probing relative in vitro gene transfer efficiencies of cationic lipids with increasing headgroup positive charges, we have designed and synthesized a series of novel mono- (**1**−**4**), di- (**5**−**7**), and trilysinated (**8**−**10**) cationic lipids. Lipids **1**−**10** were synthesized by DCC coupling of the appropriate tertiary−primary mixed amine intermediates (prepared conventionally by reacting the corresponding *N*,*N*-di-*n*-alkylamine with *N*-*tert*-butyloxycarbonyl protected 2-bromoethylamine in ethyl acetate in the presence of anhydrous potassium carbonate followed by deprotection and neutralization[2]) with appropriately protected lysine derivatives followed by acid deprotection and chloride ion exchange chromatography as outlined in Schemes 1−3. Structures of all the synthetic intermediates shown in Schemes 1−3 were confirmed by ^{1}H NMR. However, the presence of highly exchangeable protonated primary amine functions in the headgroup regions of the final lipids (**1**−**10**) caused severe line broadening of the peaks in the ^{1}H NMR spectra, particularly in the range δ 3−5 ppm. Thus, the final lipids were characterized by the molecular ion peaks in their LSIMS as well as by high-resolution mass spectrometry (HRMS−LSIMS). Unfortunately, because of their relatively high molecular weights, HRMS (LSIMS) could not be performed for lipids **8**−**10** containing trilysine headgroups. Purity of all the final lipids (**1**−**10**) was confirmed by reverse-phase analytical HPLC using two different mobile phases. As representative details, synthesis and spectral characterizations of lipids **1**, **5**, and **8** and all their intermediates (Schemes 1−3) are delineated below in the Experimental Section. Lipids **2**−**4**, **6**, **7**, **9**, and **10** were synthesized following essentially the same protocols adopted for the synthesis of lipids **1**, **5**, and **8**, respectively.

Transfection Biology. Figures 1, 2, and 3 summarize the relative in vitro gene delivery efficacies of lipids **1**−**10** in CHO, COS-1, and HepG2 cells, respectively, across the lipid/DNA charge ratios 9:1 to 0.1:1 using both DOPE and cholesterol as colipid. Several interesting and rather unexpected transfection profiles were observed. In general, lipid **1** with the myristyl tail used in combination with DOPE as colipid exhibited superior transfection properties compared to (a) the monolysinated analogues with longer hydrocarbon tails (lipids **2**−**4**), (b) the dilysine (lipids **5**−**7**) and the trilysine headgroup analogues (lipids **8**−**10**), and (c) commercially available LipofectAmine with multiple

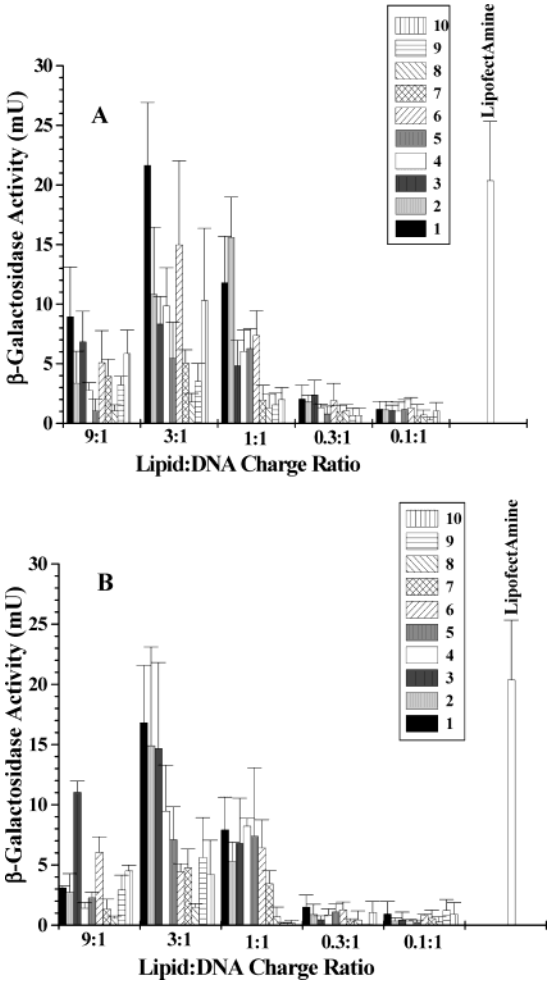

Figure 1. Transfection efficiencies of lipids **1**−**10** in CHO cells with DOPE (A) and cholesterol (B) as colipid (at 1:1 mole ratio of lipid to colipid). The transfection efficiencies of the lipids were compared to that of commercially available LipofectAmine. Transfection experiments were performed as described in the text. All the lipids were tested on the same day, and the data presented are the average of three experiments performed on three different days.

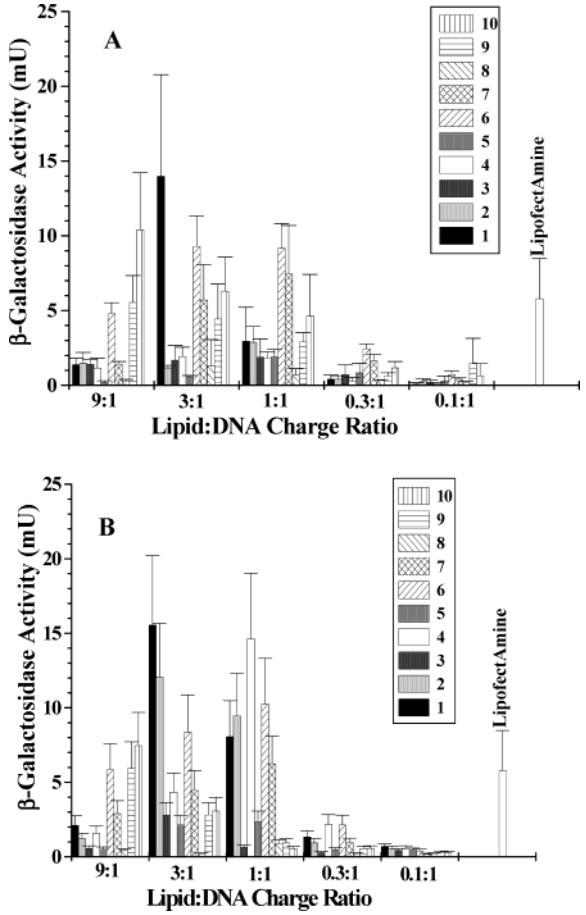

Figure 2. Transfection efficiencies of lipids **1**−**10** in COS-1 cells with DOPE (A) and cholesterol (B) as colipid (at 1:1 mole ratio of lipid to colipid). The transfection efficiencies of the lipids were compared to that of commercially available LipofectAmine. Transfection experiments were performed as described in the text. All the lipids were tested on the same day, and the data presented are the average of three experiments performed on three different days.

positive charges in its polar region (Figures 1A, 2A, and 3A). However, the transfection efficacy of lipid **1** in combination with cholesterol was seriously compromised in HepG2 cells (Figure 3B). Interestingly, monolysinated lipids with longer than myristyl tails (lipids **2** and **4**) in combination with cholesterol were found to be promising in transfecting COS-1 cells (Figure 2B). Although mono- (**1**−**4**) and dilysinated lipids (**5**−**7**) were mostly transfection-efficient at either 3:1 or 1:1 charge ratios, their transfection efficacies were comparatively less at 9:1 lipid/DNA charge ratio (Figures 1−3). In contrast, the trilysines analogues (**8**−**10**) showed their optimal gene delivery efficiencies mostly at 9:1 lipid/DNA charge ratios (Figures 1−3). All the lipids (**1**−**10**) became virtually transfection-inefficient at lipid/DNA charge ratios less than 1:1 (Figures 1−3). Similar high positive charges of the polycation/DNA complexes (thereby ensuring small and positively charged polyplexes least susceptible to possible DNase degradation) are also required for efficient cellular gene transfection mediated by cationic polymers such as polylysines.[33] However, at high polycation/DNA charge ratios, cationic polymers are, in general, toxic to cells.

An important point worth emphasizing here is that the lipofection efficacies are likely to be more influenced by the overall structure of the cationic lipids than by any specific structural features such as headgroup charge, anchor chain lengths, nature of linker group connecting polar heads and hydrophobic tails, etc. Perhaps this is why different alkyl chain lengths are required for optimal lipofection mediated by cationic lipids with varying headgroup structures.[3−5,11,30] Similarly, in the present investigation, although the optimal transfection properties for cationic lipids with monolysine headgroups (**1**-**4**) were obtained with myristyl tails, those for dilysinylated (**5**−**7**) and trilysinylated lipids (**8**−**10**) were observed with higher alkyl chain lengths (Figures 1−3). Such transfection profiles most likely owe their origin to the optimal balance of headgroup charges and the anchor hydrophobicities. A limitation of the present transfection assay with the pCMV-SPORT-β-gal plasmid carrying a β-galactosidase reporter gene is that it does not provide any information on the percent of cells transfected. In other words, an observed transfection efficiency may result either from an overall low percent of cells transfected, with few cells receiving large numbers of reporter gene, or from overall low levels of gene insertion in many cells. Taken together, the transfection results summarized in Figures 1−3 con-

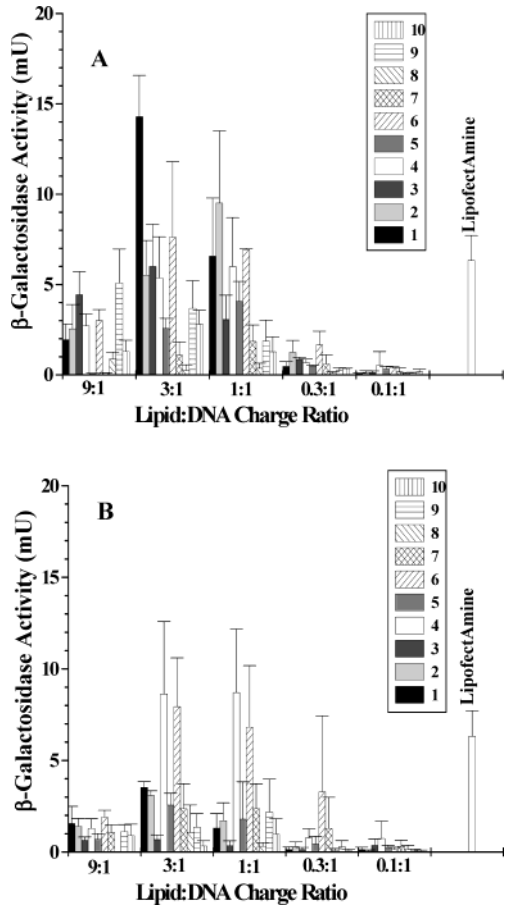

Figure 3. Transfection efficiencies of lipids **1**−**10** in HepG2 cells with DOPE (A) and cholesterol (B) as the colipid (at 1:1 mole ratio of lipid to colipid). The transfection efficiencies of the lipids were compared to that of commercially available LipofectAmine. Transfection experiments were performed as described in the text. All the lipids were tested on the same day, and the data presented are the average of three experiments performed on three different days.

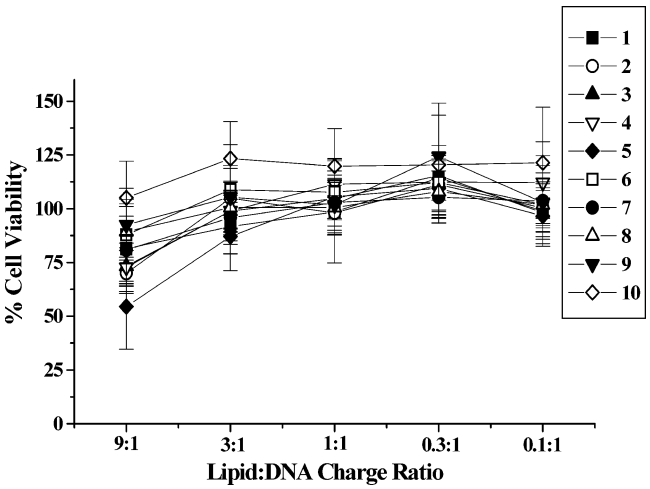

Figure 4. Representative percent cell viabilities of lipids **1**−**10** in CHO cells using MTT assay. The absorption obtained with reduced formazan with cells in the absence of lipids was taken to be 100. The toxicity assays were performed as described in the text. The data presented are the average values of three independent experiments ($n = 3$): **1** (filled square), **2** (open circle), **3** (filled triangle), **4** (open inverted triangle), **5** (filled diamond), **6** (open square), **7** (filled circle), **8** (open triangle), **9** (filled inverted triangle), **10** (open diamond).

Table 1. Representative Hydrodynamic Diameters (as Approximate Indicators of the DNA-Compacting Efficacies) of Lipoplexes Measured by Laser Light Scattering Technique[a]

	hydrodynamic diameters (nm) for the indicated lipid/DNA charge ratios		
lipid	1:1	3:1	9:1
1	107.5 ± 1.8	134.2 ± 0.7	89.8 ± 1.2
5	129.7 ± 4.5	116.9 ± 2.9	111.1 ± 7.7
8	134.7 ± 6.7	135.1 ± 1.3	90.4 ± 0.5

[a] All size measurements were done in deionized water containing 1 mM NaCl. The size of pure pDNA (without lipid) was measured to be 243.2 ± 1.2 nm. The values shown are an average of three independent measurements ($n = 3$).

vincingly demonstrate that covalent grafting of multiple positively charged functionalities in the headgroup region need not necessarily impart enhanced gene delivery efficacies to cationic lipids.

Cell Viabilities. With a view to gaining insight into whether possible higher cytotoxicities of trilysinated lipids (**8**−**10**) are at the root of their relatively lower transfection efficacies compared to their mono- (**1**−**4**) and di- (**5**−**7**) lysinated lipids, we performed the MTT-based cell viability assays for all the lipids in the representative CHO cells. The cell viability results depicted in Figure 4 clearly demonstrate that the trilysinated lipids are virtually nontoxic in the entire range of lipid/DNA charge ratios of 9:1 to 0.1:1. Cell viability of all the mono- and dicationic lipids (lipids **1**−**7**) was found to be close to 100% in the lipid/DNA charge ratio change 0.1:1 to 3:1. However, lipids **1**−**7** were found to be somewhat toxic at 9:1 lipid/DNA charge ratio (Figure 4). Such relatively higher cytotoxic nature of lipids **1**−**7** at 9:1 lipid/DNA charge ratios might play some role in reducing the efficacies of all the mono- and dilysinated lipids at 9:1 lipid/DNA charge ratios in transfecting all three cells (Figures 1−3). Taken together, the overall lower transfection properties of trilysine analogues (**8**−**10**) compared to their mono- (**1**−**4**) and dilysinated (**5**−**7**) counterparts are unlikely to originate from any differential toxicity related effects and indirectly hint at some other transfection-inhibiting parameter for lipids with trilysine headgroups (**8**−**10**).

Lipoplex Sizes and ζ Potentials. On the basis of purely electrostatic interactions, the trilysinated lipids (**8**−**10**) were anticipated to be better DNA-condensing cationic amphiphiles than their mono- (**1**−**4**) and dilysine analogues (**5**−**7**). In other words, the hydrodynamic diameters for lipoplexes prepared from lipids **8**−**10** with trilysine headgroups were expected to be smaller than lipoplexes prepared from mono- (**1**−**4**) and dilysine (**5**−**7**) counterparts. Toward obtaining approximate estimates of relative DNA-compacting efficacies of the present lipids, we measured the hydrodynamic diameters of pure plasmid DNA and some representative lipid/DNA complexes (lipoplexes) across the lipid/DNA charge ratios 9:1 to 1:1 using dynamic laser light scattering technique. Contrary to our expectation, the sizes of the lipoplexes prepared from monolysinated lipid **1** were found to be equal or smaller than the lipoplexes of the trilysine analogue (lipid **8**) across the entire range of lipid/DNA charge ratios (Table 1). At 1:1 lipid/DNA charge ratio, the hydrodynamic diameter of the lipid **1**/DNA complex (107.5 ± 1.8 nm) was found to be somewhat lower than that of lipoplexes

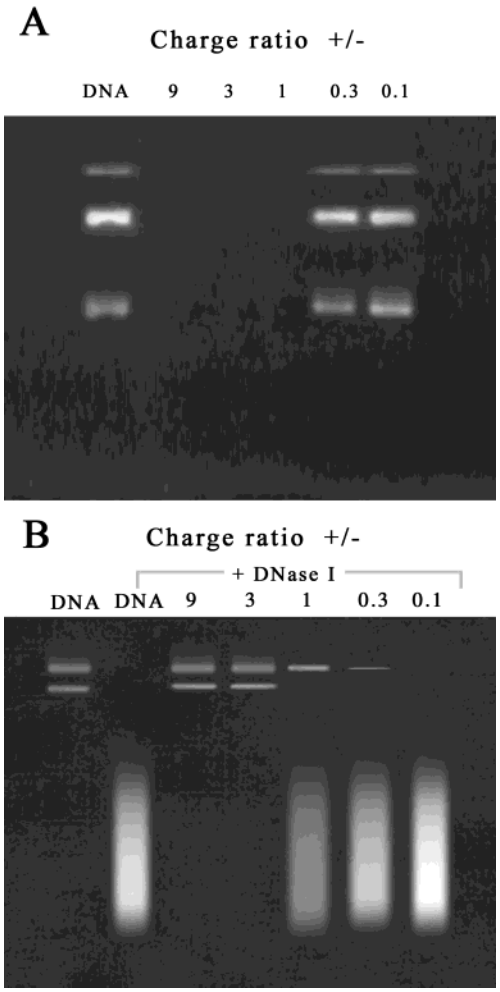

Figure 5. Gel retardation (A) and DNase I sensitivities (B) of lipoplex-associated DNA for representative lipid **5**. The lipid/DNA charge ratios are indicated at the top of each lane. The details of the treatment are as described in the text.

made from di- (**5**) and trilysine (**8**) lipids (Table 1). Strikingly, the sizes of lipid **1**/DNA complexes were essentially same as those of lipid **8**/DNA complexes at both higher lipid/DNA charge ratios of 9:1 and 3:1 (Table 1). Since the apparent sizes of all the lipoplexes were found to be similar (Table 1), lipoplex sizes are unlikely to play any key role in imparting superior transfection properties to the monolysinylated lipids. The global surface potentials of lipoplexes made from representative mono-, di-, and trilysinated lipids (**1**, **5**, and **8**, respectively) were found to be similarly negative (around −35 mV) in the presence of DMEM. Thus, surface potentials of lipid/DNA complexes are also unlikely to play any key role in modulating transfection efficacies of the presently described lysinated cationic lipids.

Lipid/DNA Binding and Lipoplex Sensitivities to DNase I. Toward initial characterization of the present lipoplexes, the electrostatic interactions between the plasmid DNA and cationic liposomes as a function of lipid/DNA charge ratios were determined by conventional electrophoretic gel retardation assay. The representative results summarized in Figure 5A demonstrate that the dilysinated cationic lipid **5** strongly binds to the plasmid DNA and completely inhibits its electrophoretic mobility at lipid/DNA charge ratio ≥ 1:1. At lipid/DNA charge ratios 0.3:1 and 0.1:1, significant amounts of free DNA were present that showed the usual electrophoretic migration into 1% agarose gel (Figure 5A). Interestingly, the same gel retardation pattern as depicted in Figure 5A for lipoplexs of dilysinated lipid **5** was also observed for representative mono- (**1**) and trilysinated (**8**) lipids (data not shown). Such similar electrophoretic mobilities of mono-, di-, and trilysinated lipids demonstrated that lipid/DNA electrostatic binding interactions are similar irrespective of the number of lysine functionalities in the headgroup region of the present cationic lipids.

The existence of substantial amounts of free DNA in the lipoplexes of all the mono-, di-, and trilysinated lipids was further confirmed by monitoring the sensitivities of the lipoplexes upon treatment with DNase I. After the free DNA digestion by DNase I, the total DNA (both the digested and inaccessible DNA) was separated from the lipid (by extracting with organic solvents) and loaded onto a 1% agarose gel. Figure 5B summarizes the results of such DNase I protection experiments for lipoplexex prepared from the representative dilysinated cationic lipid **5** across the entire lipid/DNA charge ratios of 9:1 to 0.1:1. While at high lipid/DNA charge ratios of 9:1 and 3:1, the lipoplex-associated DNA was very strongly bound to lipids and was completely inaccessible to Dnase I; increasing amounts of free DNA accessible to DNase I digestion were observed to be present in the lipoplexes as the lipid/DNA charge ratios decreased from 1:1 to 0.1:1 (Figure 5B). Interestingly, although in the gel retardation assay no free DNA was detected even at a lipid/DNA charge ratio of 1:1 (Figure 5A), significant free DNA was detected in DNase I protection experiments for the same lipid/DNA charge ratio (Figure 5B). This implies that although the lipid/DNA interaction at a 1:1 lipid/DNA charge ratio is strong enough to prevent the DNA from entering the gel, some fraction of lipoplex-associated DNA is still accessible to DNase I at the same lipid/DNA charge ratio. Once again, very similar gel patterns in DNase I protection experiments were also observed for lipoplexes of representative mono- (**1**) and trilysinated (**8**) lipids (data not shown). Similar lipid/DNA binding interactions for all the mono-, di-, and trilysinated lipids were additionally supported by the lipoplex global surface charge estimates using a dynamic laser light scattering instrument equipped with ζ-sizing capacity. Clearly, issues such as (1) the origin of the overall lower transfection efficiencies of trilysinated lipids **8**−**10** compared with those of their monolysinated counterparts (**1**−**4**) in all the three cells (Figures 1−3) despite trilysine analogues being least cytotoxic and equally DNA compacting, (2) factors leading to the dramatic fall of transfection efficacy of lipid **1** in HepG2 cells when cholesterol (and not DOPE) is used as the colipid (Figure 3), and (3) why in COS-1 cells lipids **2** and **4** are transfection-efficient only with cholesterol (and not DOPE) as colipid (Figure 2) remain elusive at this stage of investigation.

In summary, evaluating the in vitro gene delivery efficacies of a series of novel cationic lipids with mono-, di-, and trilysine headgroups and a common hydrophobic anchor skeleton (lipids **1**−**10**, Schemes 1−3), we have demonstrated, for the first time, that the monolysine lipid with a myristyl tail exhibits superior transfection efficacies compared to its di- and trilysine analogues in

CHO, COS-1, and HepG2 cells. Contrary to popular belief, our lipoplex size data indicate that singly lysinated cationic amphiphiles can also be better or equally DNA-compacting than their di- and trilysine counterparts. Both gel retardation and DNase I sensitivity assays indicated similar lipid/DNA binding interactions for all the novel mono-, di-, and trilysinated cationic lipids. Taken together, the present findings support the notion that caution needs to be exercised in ensuring enhanced gene delivery efficacies of cationic lipids through covalent grafting of multiple lysine functionalities in the headgroup region.

Experimental Section

General Procedures and Materials. The high-resolution mass spectrometric (HRMS) analyses were performed on a Micromass AUTOSPEC-M mass spectrometer (Manchester, U.K.) with an OPUS V3 1X data system. Data were acquired by the liquid secondary ion mass spectrometry (LSIMS) technique using *m*-nitrobenzyl alcohol as the matrix. LSIMS analysis was performed in the scan range 100−1000 amu at a rate of 3 scans/s. ^{1}H NMR spectra were recorded on a Varian FT 200 MHz, AV 300 MHz, or Varian Unity 400 MHz spectrometer. 1-Bromotetradecane, 1-bromohexadecane, 1-bromooctadecane, *n*-tetradecylamine, *n*-hexadecylamine, and *n*-octadecylamine were procured from Lancaster (Morecambe, England). Oleylamine was purchased from Fluka (Switzerland), and L-lysine and N^{α}-Z-L-lysine were purchased from Aldrich. The progress of the reactions was monitored by thin-layer chromatography on 0.25 mm silica gel plates. Column chromatography was performed with silica gel (Acme Synthetic Chemicals, India, finer than 200 and 60−120 mesh). *p*-CMV-SPORT-*β*-gal plasmid was a generous gift from Dr. Nalam Madhusudhana Rao. LipofectAmine was purchased from Invitrogen life technologies. Cell culture media, fetal bovine serum, 3-(4,5-dimethylthiazol-2-yl)-2,5-diphenyltetrazolium bromide (MTT), poly(ethylene glycol) 8000, *o*-nitrophenyl-*β*-D-galactopyranoside, and cholesterol were purchased from Sigma (St. Louis, MO). NP-40, antibiotics, and agarose were purchased from Hi-media, India. DOPE was purchased from Fluka (Switzerland). Unless otherwise stated, all the other reagents purchased from local commercial suppliers were of analytical grade and were used without further purification. COS-1 (SV 40 transformed African green monkey kidney cells), CHO (Chinese hamster ovary), and HepG2 (human hepatocarcinoma) cell lines were procured from the National Centre for Cell Sciences (NCCS), Pune, India. Cells were grown at 37 °C in Dulbecco's modified Eagle's medium (DMEM) with 10% FBS in a humidified atomosphere containing 5% CO_2/95% air. The purity of all the final lipids (**1**−**10**) was determined by analytical HPLC (Shimadzu model LC10A) using a PARTISIL 5 ODS-3 WCS analytical column (4.6 mm × 250 mm, Whatman Inc., Clifton, NJ) in two different mobile phases. One solvent system (A) was methanol/acetonitrile/water/trifluoroacetic acid in the ratio 65:10:25:0.05 (v/v) for 15 min with a flow rate of 0.8 mL/min. The other solvent system (B) was methanol:water:trifluoroacetic acid in the ratio 75:25:0.05 for 15 min with a flow rate of 0.8 mL/min. Peaks were detected by UV absorption at 219 nm. All the target lipids (**1**−**10**) showed more than 95% purity. Typical retention times in mobile phase B were 3.54 min (lipid **1**), 3.60 min (lipid **2**), 3.59 min (lipid **3**), 3.58 min (lipid **4**), 3.65 min (lipid **5**), 3.57 min (lipid **6**), 3.86 min (lipid **7**), 3.55 mins (lipid **8**), 3.65 min (lipid **9**), and 3.56 min (lipid **10**).

Synthesis. As representative examples, details of the synthetic procedures are provided below for lipids **1**, **5**, and **8**. Lipids **2**−**4**, **6** and **7**, and **9** and **10** were synthesized following the same protocol as those for lipids **1**, **5**, and **8**, respectively. Because of extensive line broadening in ^{1}H NMR spectra of all the final deprotected lipids (particularly in the region δ/ppm = 3−5), all the final lipids were characterized by LSIMS and HRMS (LSIMS). However, ^{1}H NMR spectra of the BOC-protected immediate precursors for all the final lipids (provided below) were in complete agreement with their molecular structures (Schemes 1−3).

Synthesis of DTMLAC (Lipid 1, Scheme 1). Step a. Solid HOSu (0.20 g, 1.73 mmol) and DCC (0.36 g, 1.73 mmol) were added sequentially to an ice-cold and stirred solution of N^{α},N^{ϵ}-di-*tert*-butyloxycarbonyl-L-lysine (0.6 g, 1.73 mmol, prepared from L-lysine and di-*tert*-butyldicarbonate as described previously[34]) in dry DCM/dry DMF (9:1, v/v). After half an hour, *N*-aminoethyl-*N*,*N*-di-*n*-tetradecylamine (**I**, 0.65 g, 1.44 mmol, prepared as described previously[31]) and DMAP (catalytic) dissolved in dry DCM were added to the reaction mixture. The resulting solution was left stirred at room temperature for 24 h, solid DCU was filtered, and the solvent from the filtrate was evaporated. The residue was taken in ethyl acetate (100 mL) and washed sequentially with ice-cooled 1 N HCl (3 × 100 mL), saturated sodium bicarbonate (3 × 100 mL), and water (3 × 100 mL). The organic layer was dried over anhydrous sodium sulfate and filtered, and the solvent from the filtrate was removed by rotary evaporation. The residue upon column chromatographic purification with 60−120 mesh silica gel using 1−2% methanol/dichloromethane (v/v) as eluent afforded 0.8 g (71.4%) of the pure intermediate *N*-2-[*N*′-(N^{α},N^{ϵ}-di-BOC-L-Lysyl)]aminoethyl-*N*,*N*-di-*n*-tetradecylamine (R_f = 0.55, 5% methanol/dichloromethane, v/v). ^{1}H NMR (200 MHz, $CDCl_3$): δ/ppm = 0.9 [t, 6H, CH_3−$(CH_2)_{11}$−], 1.2−1.4 [bs, 44H, −$(CH_2)_{11}$−], 1.3−1.6 [m, 4H, LysC$^{\gamma}H_2$ + LysC$^{\delta}H_2$], 1.4 [s, 9H,-CO−O−C(CH_3)$_3$], 1.45 [m, 4H, −N(−CH_2−CH_2−)$_2$], 1.7 [m, 2H, LysC$^{\beta}H_2$], 2.4 [t, 4H, −N(−CH_2−CH_2−)$_2$], 2.5 [t, 2H, −N−CH_2−CH_2− NH−CO], 3.1 [m, 2H, Lys$^{\omega}CH_2$], 3.3 [m,2H, −N−CH_2−CH_2−NH−CO−O−], 4.0 [m, 1H, LysC$^{\alpha}H$], 4.6 [m, 1H, BOC −N*H*], 5.1 (m, 1H, Boc−N*H*), 6.8 [m, 1H, −CH_2−CH_2−N*H*−CO−O−].

Step b. The intermediate obtained in step a was dissolved in 3 mL of dichloromethane/methanol (2:1, v/v), and 3 mL of methyl iodide was added. The solution was stirred at room temperature overnight. Solvent was removed on a rotary evaporator. The residue upon column chromatographic purification with 60−120 mesh size silica gel and 2−3% methanol in dichloromethane (v/v) as eluent afforded 0.7 g (88.7% yield) of the intermediate *N*-2-[*N*′-(N^{α},N^{ϵ}−di-BOC-L-Lysyl)]aminoethyl-*N*,*N*-di-*n*-tetradecyl-*N*-methylammonium iodide (R_f = 0.45, 5% methanol in dichloromethane, v/v). ^{1}H NMR (200 MHz, $CDCl_3$): δ/ppm = 0.9 [t, 6H, CH_3−$(CH_2)_{11}$−], 1.2−1.4 [bs, 44H, −$(CH_2)_{11}$−], 1.3−1.6 [m, 4H, LysC$^{\gamma}H_2$ + LysC$^{\delta}H_2$], 1.4 [s, 9H, −CO−O−C(CH_3)$_3$], 1.6−1.8 [m, 4H, −N$^+$(−CH_2−CH_2−)$_2$], 1.7 [m, 2H, LysC$^{\beta}H_2$], 3.1 [m, 2H, Lys$^{\omega}CH_2$], 3.3 [s, 3H,−N$^+$ −CH_3], 3.4−3.5 [m, 4H, −N$^+$(−CH_2−CH_2−)$_2$], 3.7 [m, 4H, −N$^+$−CH_2−CH_2−NH−CO−O], 4.1 [m, 1H, LysC$^{\alpha}H$], 4.8 [m, 1H, BOC −N*H*], 5.5 [m, 1H, BOC−N*H*], 8.2 [m, 1H, −CH_2−CH_2−N*H*−CO−O−].

Steps c and d. The intermediate obtained in step b (0.7 g, 0.76 mmol) was dissolved in dry DCM (2 mL), and TFA (2 mL) was added at 0 °C. The resulting solution was left stirred at room temperature overnight to ensure complete deprotection. Excess TFA was removed by flushing nitrogen to give the title compound as a trifluoroacetate salt. Column chromatographic purification using 60−120 mesh size silica gel and 10−12% (v/v) methanol/chloroform as eluent followed by chloride ion exchange chromatography (using amberlyst A-26 chloride ion exchange resin) afforded 0.26 g (36.5% yield) of the pure title compound (DTMLAC, R_f = 0.2, 20% methanol in chloroform, v/v). LSIMS (lipid **1**): *m*/*z* 596 [M$^+$] (calcd for $C_{37}H_{79}ON_4$, 100%). HRMS (LSIMS, lipid **1**): *m*/*z* (for $C_{37}H_{79}ON_4$, 100%) 595.6254; found 595.6332.

DHMLAC (Lipid 2). ^{1}H NMR (200 MHz, $CDCl_3$) of *N*-2-[*N*′-(N^{α},N^{ϵ}-di-BOC-L-Lysyl)]aminoethyl-*N*,*N*-di-*n*-hexadecyl-*N*-methylammonium iodide (immediate precursor of lipid **2**): δ/ppm = 0.9 [t, 6H, CH_3−$(CH_2)_{13}$−], 1.2−1.4 [bs, 52H, −$(CH_2)_{13}$−], 1.3−1.6 [m, 4H, LysC$^{\gamma}H_2$ + LysC$^{\delta}H_2$], 1.4 [s, 9H, −CO−O−C(CH_3)$_3$], 1.6−1.9 [m, 6H, −N$^+$(−CH_2−CH_2−)$_2$ + LysC$^{\beta}H_2$], 3.1 [m, 2H, Lys$^{\omega}CH_2$], 3.3 [s, 3H, −N$^+$−CH_3], 3.4−3.5 [m, 4H, −N$^+$-(−CH_2−CH_2−)$_2$], 3.8 [m,4H, −N$^+$−CH_2−CH_2−NH−CO−O], 4.1 [m, 1H, LysC$^{\alpha}H$], 4.8 [m, 1H, BOC−N*H*], 5.45 [m, 1H,

BOC−N*H*], 8.3 [m, 1H, −CH_2−CH_2−N*H*−CO−O−]. LSIMS: *m/z* 651 [M^+] (calcd for $C_{41}H_{87}ON_4$ 4^0 ammonium ion, 100%). HRMS (LSIMS): *m/z* (for $C_{41}H_{87}ON_4$, 4^0 ammonium ion, 100%) 651.6880; found 651.6841.

DOMLAC (Lipid 3). ^{1}H NMR (200 MHz, $CDCl_3$) of *N*-2-[*N*′-(N^α,N^ϵ-di-BOC-L-Lysyl)]aminoethyl-*N*,*N*-di-*n*-octadecyl-*N*-methylammonium iodide (immediate precursor of lipid **3**): δ/ppm = 0.9 [t, 6H, C*H*$_3$−$(CH_2)_{15}$−], 1.2−1.4 [bs, 60H, −$(CH_2)_{15}$−], 1.3−1.6 [m, 4H, LysC$^\gamma H_2$ + LysC$^\delta H_2$], 1.4 [s, 9H, −CO−O−C$(CH_3)_3$], 1.6−1.85 [m, 6H, $-N^+(-CH_2-CH_2-)_2$ + LysC$^\beta H_2$], 3.1 [m, 2H, Lys$^\omega CH_2$], 3.3 [s, 3H, $-N^+-CH_3$], 3.4−3.5 [m, 4H, $-N^+(-CH_2-CH_2-)_2$], 3.7 [m,4H, $-N^+-CH_2-CH_2-$NH−CO−O], 4.1 [m, 1H, LysC$^\alpha H$], 4.85 [m, 1H, BOC −N*H*], 5.45 [m, 1H, BOC−N*H*], 8.25 [m, 1H, −CH_2−CH_2−N*H*−CO−O−]. LSIMS: *m/z* 708 [M^+] (calcd for $C_{45}H_{97}ON_4$, 4^0 ammonium ion, 40%). HRMS (LSIMS): *m/z* (for $C_{45}H_{97}ON_4$, 4^0 ammonium ion 100%) 707.7506; found 707.7466.

OOLAC (Lipid 4). ^{1}H NMR (300 MHz, $CDCl_3$) of *N*-2-[*N*′-(N^α,N^ϵ-di-BOC-L-Lysyl)]-*N*-*n*-octadecyl-*N*-oleyl-*N*-methylammonium iodide (immediate precursor of lipid **4**): δ/ppm = 0.9 [t, 6H, C*H*$_3$−$(CH_2)_{17}$−], 1.2−1.4 [bs, 52H, −$(CH_2)_{13}$−], 1.3−1.6 [m, 4H, LysC$^\gamma H_2$ + LysC$^\delta H_2$], 1.4 [s, 9H, −CO−O−C$(CH_3)_3$], 1.6−1.85 [m, 6H, $-N^+(-CH_2-CH_2-)_2$ + LysC$^\beta H_2$], 1.90−2.20- [m, 4H, −CH_2−CH=CH−CH_2−], 3.1 [m, 2H, Lys$^\omega CH_2$], 3.3 [s, 3H, $-N^+-CH_3$], 3.4−3.5 [m, 4H, $-N^+(-CH_2-CH_2-)_2$], 3.8 [m, 4H, $-N^+-CH_2-CH_2-$NH−CO−O], 4.1 [m, 1H, LysC$^\alpha H$], 4.8 [m, 1H, BOC−N*H*], 5.30 [t, 2H, −CH_2−CH=CH−CH_2−], 5.45 [m, 1H, BOC−N*H*], 8.3 [m, 1H, −CH_2−CH_2−N*H*−CO−O−]. LSIMS: *m/z* 705 [M^+] (calcd for $C_{45}H_{95}ON_4$, 4^0 ammonium ion, 100%). HRMS (LSIMS): *m/z* (for $C_{45}H_{95}ON_4$, 4^0 ammonium ion, 100%) 705.7349; found 705.7347.

Synthesis of DTML$_2$AC (Lipid 5, Scheme 2). Step a. N^ϵ-*tert*-Butyloxycarbonyl-N^α-benzyloxycarbonyl-L-lysine (3.63 g, 9.53 mmol, prepared from N^α-benzyloxycarbonyl-L-lysine and ditertiarybutyl dicarbonate as described previously[34]) and *N*-aminoethyl-*N*,*N*-di-*n*-tetradecylamine (**I**, 3.59 g, 7.94 mmol) were coupled in the presence of DCC (1.96 g, 9.53 mmol), solid HOSu (1.1 g, 9.53 mmol), DMAP (catalytic) following essentially the same protocol as described above in step a of the DTMLAC synthesis. The resulting crude product upon column chromatographic purification with 60−120 mesh silica gel and 7% acetone in petroleum ether (v/v) as eluent afforded 4.43 g (76.8%) of the pure intermediate *N*-2-[*N*′-(N^α-Z-N^ϵ-BOC-L-Lysyl)]aminoethyl-*N*,*N*-di-*n*-tetradecylamine as a white solid. (R_f = 0.43, 30% acetone in petroleum ether, v/v). ^{1}H NMR (200 MHz, $CDCl_3$): δ/ppm = 0.9 [t, 6H, C*H*$_3$−$(CH_2)_{11}$−], 1.2−1.4 [bs, 44H, −$(CH_2)_{11}$−], 1.3−1.6 [m, 4H, LysC$^\gamma H_2$ + LysC$^\delta H_2$], 1.4 [s, 9H, −CO−O−C$(CH_3)_3$], 1.45 [m, 4H, $-N(-CH_2-CH_2-)_2$], 1.7[m, 2H, LysC$^\beta H_2$], 2.4 [t, 4H, $-N(-CH_2-CH_2-)_2$], 2.5 [t, 2 H,−N−CH_2−CH_2−NH−CO−O−], 3.1 [m, 2H, Lys$^\omega CH_2$], 3.3 [m, 2H, −N−CH_2−CH_2−NH−CO−O−], 4.1 [m, 1H, LysC$^\alpha H$], 4.6 [m, 1H, BOC−N*H*], 5.1 (s, 2H, Z-CH_2), 5.5 (m, 1H, Z−N*H*), 6.8 [m, 1H, −CH_2−CH_2−N*H*−CO−], 7.3 (s, 5H, Ar−*H*).

Step b. The intermediate (1 g, 1.23 mmol) obtained in step a was dissolved in dry methanol (10 mL) containing a few drops of glacial acetic acid. Ammonium formate (0.39 g, 6.14 mmol) and 10% Pd/C (0.25 g) were added, and the reaction mixture was allowed to stir under nitrogen atmosphere for 4 h. The catalyst was removed by filtration through Celite, and the filtrate was evaporated to dryness. The residue was taken in ethyl acetate (50 mL) and washed sequentially with 30% aqueous potassium carbonate (3 × 50 mL), saturated sodium chloride (3 × 50 mL), and water (3 × 50 mL). The organic layer was dried over anhydrous sodium sulfate and filtered, and rotatory evaporation of the solvent from the filtrate afforded 0.7 g (83.8%) of the intermediate *N*-2-[*N*′-(N^ϵ-BOC-L-Lysyl)]-aminoethyl-*N*,*N*-di-*n*-tetradecylamine (**II**, Scheme 2) as a pure white solid (R_f = 0.2, 5% methanol in dichloromethane, v/v). ^{1}H NMR (200 MHz, $CDCl_3$): δ/ppm = 0.9 [t, 6H, C*H*$_3$−$(CH_2)_{11}$−], 1.2−1.4 [bs, 44H, −$(CH_2)_{11}$−], 1.3−1.6 (m, 4 H, LysC$^\gamma H_2$ + LysC$^\delta H_2$), 1.4 (s, 9H, CO−O−C$(CH_3)_3$, 1.45 [m, 4H, $-N(-CH_2-CH_2-)_2$], 1.7 (m, 2H, LysC$^\beta H_2$), 2.4 [t, 4H, $-N(-CH_2-CH_2-)_2$], 2.5 (t, 2 H,−N−CH_2−CH_2− NH−CO], 3.1 (m, 2H, Lys$^\omega CH_2$), 3.2−3.3 [m, 3H, −N−CH_2−CH_2−NH−CO and LysC$^\alpha H$], 4.5 [m, 1H, BOC−N*H*], 7.5 [m, 1H, −CH_2−CH_2−N*H*−CO−].

Step c. N^α,N^ϵ-di-*tert*-Butyloxycarbonyl-L-lysine (0.38 g, 1.10 mmol) was coupled with intermediate **II** (0.63 g, 0.92 mmol, prepared above in step b) in the presence of solid HOSu (0.13 g, 1.10 mmol), DCC (0.23 g, 1.10 mmol), and DMAP (catalytic) following essentially the same protocol as described above in step a of the DTMLAC synthesis. The resulting crude product upon column chromatographic purification with 60−120 mesh silica gel and 10% acetone in petroleum ether (v/v) as eluent afforded 0.74 g (79.7% yield) of the pure compound *N*-2-[*N*′-(N^α,N^ϵ-di-BOC-L-Lys-N^ϵ-BOC-L-Lys)]aminoethyl-*N*,*N*-di-*n*-tetradecylamine as a white gummy solid. (R_f = 0.42, 30% acetone in pet-ether, v/v). ^{1}H NMR (200 MHz, $CDCl_3$): δ/ppm = 0.9 [t, 6H, C*H*$_3$−$(CH_2)_{11}$−], 1.2−1.4 [bs, 44H, −$(CH_2)_{11}$−], 1.3−1.9 [m, 16H, LysC$^\beta H_2$ + LysC$^{\beta'} H_2$ + LysC$^\gamma H_2$ + LysC$^{\gamma'} H_2$ + LysC$^\delta H_2$ + LysC$^{\delta'} H_2$ + $-N(-CH_2-CH_2-)_2$], 1.4 [s, 27H, CO−O−C$(CH_3)_3$], 2.4 [t, 4H, $-N(-CH_2-CH_2-)_2$], 2.5 (t, 2H,−N−CH_2−CH_2−NH−CO], 3.1 [m, 4H, Lys$^\omega CH_2$ + Lys$^{\omega'} CH_2$], 3.3 [m, 2H,−N−CH_2−CH_2−NH−CO−], 4.1 [m, 1H, LysC$^\alpha H$], 4.3 [m, 1H, LysC$^{\alpha'} H$], 4.8 [m, 2H, BOC−N*H*], 5.4 [m, 1H, BOC−N*H*], 6.6 [m, 1H, CH_2−CH_2−N*H*−CO−], 6.8 [m, 1H, −CO−CH−N*H*−CO−].

Step d. The intermediate obtained in step c (0.74 g, 0.73 mmol) was dissolved in 3 mL of dichloromethane/methanol (2:1, v/v), and 3 mL of methyl iodide was added. The solution was stirred at room temperature overnight, and the solvent was removed on a rotary evaporator. The residue upon column chromatographic purification with 60−120 mesh size silica gel and 32% acetone in petroleum ether (v/v) as eluent afforded 0.37 g (57.2% yield) of intermediate *N*-2-[*N*′-(N^α,N^ϵ-di-BOC-L-Lys-N^ϵ-BOC-L-Lys)]aminoethyl-*N*,*N*-di-*n*-tetradecyl-*N*-methylammonium iodide as a white gummy solid (R_f = 0.24, 30% acetone in pet ether, v/v). ^{1}H NMR (200 MHz, $CDCl_3$): δ/ppm = 0.9 [t, 6H, C*H*$_3$−$(CH_2)_{11}$−], 1.2−1.4 [bs, 44H, −$(CH_2)_{11}$−], 1.3−2.0 [m, 16H, LysC$^\beta H_2$ + LysC$^{\beta'} H_2$ + LysC$^\gamma H_2$ + LysC$^{\gamma'} H_2$ + LysC$^\delta H_2$ + LysC$^{\delta'} H_2$ + $-N^+(-CH_2-CH_2-)_2$], 1.4 [s, 27H, CO−O−C$(CH_3)_3$], 3.1 [m, 4H, Lys$^\omega CH_2$ + Lys$^{\omega'} CH_2$], 3.3 [s, 3H, $-N^+-CH_3$], 3.4 [m, 4H, $-N^+(-CH_2-CH_2-)_2$], 3.7 [m, 4H, $-N^+-CH_2-CH_2-$NH−CO], 4.1 [m, 1H, LysC$^\alpha H$], 4.3 [m, 1H, LysC$^{\alpha'} H$], 4.9 [m, 2H, BOC−N*H*], 5.4 (m, 1H, BOC−N*H*), 7.2 [m, 1H, CH_2−CH_2−N*H*−CO−], 8.2 [m, 1H, −CO−CH−N*H*−CO−].

Steps e and f. The compound obtained in step d (0.36 g, 0.32 mmol) was dissolved in dry DCM (2 mL), and TFA (2 mL) was added at 0 °C. The resulting solution was left stirred at room temperature overnight to ensure complete deprotection. Excess TFA was removed by flushing nitrogen to give the title compound as a trifluoroacetate salt. Repeated crystallization from diethyl ether/methanol (4:1) followed by chloride ion exchange chromatography (using Amberlyst A-26 chloride ion exchange resin) afforded 0.21 g (55.5% yield) of the pure title compound DTML$_2$AC (R_f = 0.15, 20% methanol/dichloromethane, v/v). LSIMS (lipid **5**): *m/z* 723 [M^+] (calcd for $C_{43}H_{91}O_2N_6$, 4^0 ammonium ion, 10%). HRMS (LSIMS, lipid **5**): *m/z* (for $C_{43}H_{91}O_2N_6$, 4^0 ammonium ion, 100%) 723.7184; found 723.7204.

DHML$_2$AC (Lipid 6). ^{1}H NMR (200 MHz, $CDCl_3$) of *N*-2-[*N*′-(N^α,N^ϵ-di-BOC-L-Lys-N^ϵ-BOC-L-Lys)]aminoethyl-*N*,*N*-di-*n*-hexadecyl-*N*-methylammonium iodide (immediate precursor of lipid **6**): δ/ppm = 0.9 [t, 6H, C*H*$_3$−$(CH_2)_{13}$−], 1.2−1.4 [bs, 52H, −$(CH_2)_{13}$−], 1.3−1.6 [m, 8H, LysC$^\gamma H_2$ + LysC$^{\gamma'} H_2$ + LysC$^\delta H_2$ + LysC$^{\delta'} H_2$], 1.4 [s, 27H, CO−O−C$(CH_3)_3$], 1.6−1.8 [m, 4H, $-N^+(-CH_2-CH_2-)_2$], 2.0−2.2 [m, 4H, LysC$^\beta H_2$ + LysC$^{\beta'} H_2$], 3.1 [m, 4H, Lys$^\omega CH_2$ + Lys$^{\omega'} CH_2$], 3.3 [s, 3H, $-N^+-CH_3$], 3.4 [m, 4H, $-N^+(-CH_2-CH_2-)_2$], 3.7 [m, 4H, $-N^+-CH_2-CH_2-$NH−CO], 4.1 [m, 1H, LysC$^\alpha H$], 4.3 [m, 1H, LysC$^{\alpha'} H$], 5.0 [m, 2H, BOC−N*H*], 5.65 (m, 1H, BOC−N*H*), 7.35 [m, 1H, CH_2−CH_2−N*H*−CO−], 8.25 [m, 1H, −CO−CH−N*H*−CO−]. LSIMS: *m/z* 780 [M^+] (calcd for $C_{47}H_{99}O_2N_6$, 4^0 ammonium ion, 70%). HRMS (LSIMS): *m/z* (for for $C_{47}H_{99}O_2N_6$, 4^0 ammonium ion, 100%) 779.7830; found 779.7893.

DOML$_2$AC (Lipid 7). ^{1}H NMR (200 MHz, $CDCl_3$) of *N*-2-[*N*′-(N^α,N^ϵ-di-BOC-L-Lys-N^ϵ-BOC-L-Lys)]aminoethyl-*N*,*N*-di-*n*-

octadecyl-*N*-methylammonium iodide (immediate precursor of lipid **7**): δ/ppm = 0.9 [t, 6H, $CH_3-(CH_2)_{15}-$], 1.2−1.4 [bs, 60H, $-(CH_2)_{15}-$], 1.3−2.0 [m, 16H, LysC$^{\beta}H_2$ + LysC$^{\beta'}H_2$ + LysC$^{\gamma}H_2$ + LysC$^{\gamma'}H_2$ + LysC$^{\delta}H_2$ + LysC$^{\delta'}H_2$ + $-N^+(-CH_2-CH_2-)_2$], 1.4 [s, 27H, CO−O−C(CH_3)$_3$], 3.1 [m, 4H, Lys$^{\omega}CH_2$ + Lys$^{\omega'}CH_2$], 3.3 [s, 3H, $-N^+-CH_3$], 3.4 [m, 4H, $-N^+(-CH_2-CH_2-)_2$], 3.7 [m, 4H, $-N^+-CH_2-CH_2-NH-CO$], 4.1 [m, 1H, LysC$^{\alpha}H$], 4.3 [m, 1H, LysC$^{\alpha'}H$], 5.0 [m, 2H, BOC N*H*], 5.65 (m, 1H, BOC N*H*), 7.35 [m, 1H, $CH_2-CH_2-NH-CO-$], 8.25 [m, 1H, $-CO-CH-NH-CO-$]. LSIMS: *m*/*z* 836 [M$^+$] (calcd for $C_{51}H_{107}O_2N_6$, 4^0 ammonium ion, 75%). HRMS (LSIMS): *m*/*z* (for $C_{51}H_{107}O_2N_6$, 4^0 ammonium ion, 100%) 835.8581; found 835.8576.

Synthesis of DTML$_3$AC (Lipid 8, Scheme 3). Steps a and b. The synthesis is the same as steps a and b described above for preparing intermediate **II** in DTML$_2$AC synthesis.

Step c. N^{ϵ}-*tert*-Butyloxycarbonyl-N^{α}-benzyloxycarbonyl-L-lysine (0.87 g, 2.29 mmol) was coupled with intermediate **II** (1.3 g, 1.91 mmol) in the presence of solid HOSu (0.27 g, 2.29 mmol), DCC (0.47 g, 2.29 mmol), and DMAP (catalytic) following essentially the same protocol as described above in step a of the DTMLAC synthesis. The resulting crude product upon column chromatographic purification with 60−120 mesh silica gel using 2.2% methanol in dichloromethane (v/v) as eluent afforded 1.55 g (77.9% yield) of *N*-2-[*N*′-(N^{α}-Z,N^{ϵ}-BOC-L-Lys-N^{ϵ}-BOC-L-Lys)]aminoethyl-*N*,*N*-di-*n*-tetradecylamine as a gummy solid (R_f = 0.37, 30% acetone in petroleum ether, v/v). ^{1}H NMR (200 MHz, CDCl$_3$): δ/ppm = 0.9 [t, 6H, $CH_3-(CH_2)_{11}-$], 1.2−1.4 [bs, 44H, $-(CH_2)_{11}-$], 1.3−1.9 [m, 16H, LysC$^{\beta}H_2$ + LysC$^{\beta'}H_2$ + LysC$^{\gamma}H_2$ + LysC$^{\gamma'}H_2$ + LysC$^{\delta}H_2$ + LysC$^{\delta'}H_2$+ $-N(-CH_2-CH_2-)_2$], 1.4 [s, 18H, CO−O−C(CH_3)$_3$], 2.4 [t, 4H, $-N(-CH_2-CH_2-)_2$, 2.5 [t, 2H, $-N-CH_2-CH_2-NH-CO-$], 3.1 [m, 4 H, Lys$^{\omega}CH_2$ + Lys$^{\omega'}CH_2$], 3.3 [t, 2 H, $-N-CH_2-CH_2-NH-CO-$], 4.2 [m, 1H, LysC$^{\alpha}H$], 4.4 [m, 1H, LysC$^{\alpha'}H$], 4.9 [m, 2H, BOC N*H*], 5.1 (s, 2H, Z−CH_2), 5.9 [m, 1H, Z−N*H*], 6.7 [m, 1H, $-CH_2-CH_2-NH-CO-$], 7.0 [m, 1H, $-CO-CH-NH-CO-$], 7.3 [s, 5H, Ar−*H*].

Step d. The compound prepared in step c (1.53 g, 1.47 mmol) was dissolved in dry methanol (10 mL) containing a few drops of glacial acetic acid. Ammonium formate (0.46 g, 7.34 mmol) and 10% Pd/C (0.38 g) were added to the solution, and the reaction mixture was allowed to stir under a nitrogen atmosphere for 4 h to ensure complete hydrogenolysis. The catalyst was removed by filtration through Celite, and the filtrate was evaporated to dryness. The residue was taken in ethyl acetate (50 mL) and washed sequentially with 30% aqueous potassium carbonate (3 × 50 mL), saturated sodium chloride (3 × 50 mL), and water (3 × 50 mL). The organic layer was dried over anhydrous sodium sulfate, and the filtrate was evaporated in a vacuum to afford 0.1.09 g (81.9%) of pure *N*-2-[*N*′-(N^{ϵ}-BOC-L-Lys-N^{ϵ}-BOC-L-Lys)]aminoethyl-*N*,*N*-di-*n*-tetradecylamine as a white gummy solid (R_f = 0.14, 5% methanol in dichloromethane, v/v). ^{1}H NMR (200 MHz, CDCl$_3$): δ/ppm = 0.9 [t, 6H, $CH_3-(CH_2)_{11}-$], 1.2−1.4 [bs, 44H, $-(CH_2)_{11}-$], 1.3−1.9 [m, 16H, LysC$^{\beta}H_2$ + LysC$^{\beta'}H_2$ + LysC$^{\gamma}H_2$ + LysC$^{\gamma'}H_2$ + LysC$^{\delta}H_2$ + N($-CH_2-CH_2-$)$_2$], 1.4 [s, 18H, $-CO-O-C(CH_3)_3$], 2.4 [t, 4H, $-N(-CH_2-CH_2-)_2$,], 2.5 (t, 2H, $-N-CH_2-CH_2-NH-CO-$], 3.1 [m, 4H, Lys$^{\omega}CH_2$ + Lys$^{\omega'}CH_2$], 3.2−3.4 [m, 3H, $-N-CH_2-CH_2-NH-CO-$ + LysC$^{\alpha}H$], 4.3 [m, 1H, LysC$^{\alpha'}H$], 4.7 [m, 2H, BOC N*H*], 6.6 [m, 1H, $-CH_2-CH_2-NH-CO-$], 7.7 [m, 1H, $-CO-CH-NH-CO-$].

Step e. N^{α},N^{ϵ}-Di-*tert*-butyloxycarbonyl-L-lysine (0.5 g, 1.44 mmol) was coupled with the intermediate prepared above in step d (1.09 g, 1.2 mmol) in the presence of solid HOSu (0.17 g, 1.44 mmol), DCC (0.3 g, 1.44 mmol), and DMAP (catalytic) following essentially the same protocol as described above in step a of the DTMLAC synthesis. The resulting crude product upon column chromatographic purification with 60−120 mesh silica gel using 4% methanol in dichloromethane (v/v) as eluent afforded 1.0 g (67.4% yield) of *N*-2-[*N*′-(N^{α},N^{ϵ}-di-BOC-L-Lys-N^{ϵ}-BOC-L-Lys-N^{ϵ}-BOC-L-Lys)]aminoethyl-*N*,*N*-di-*n*-tetradecylamine interemediate as a gummy solid (R_f = 0.35, 30% acetone in petroleum ether, v/v). ^{1}H NMR (200 MHz, CDCl$_3$): δ/ppm = 0.9 [t, 6H, $CH_3-(CH_2)_{11}-$], 1.2−1.4 [bs, 44H, $-(CH_2)_{11}-$], 1.4−1.9 (m, 22H, LysC$^{\beta}H_2$ + LysC$^{\beta'}H_2$ + LysC$^{\beta''}H_2$ + LysC$^{\gamma}H_2$ + LysC$^{\gamma'}H_2$ + LysC$^{\gamma''}H_2$ + LysC$^{\delta}H_2$ + LysC$^{\delta'}H_2$ + LysC$^{\delta''}H_2$ + $-N(-CH_2-CH_2-)_2$], 1.4 [s, 36H, $-CO-O-C(CH_3)_3$], 2.4 [t, 4H, $-N(-CH_2-$ $CH_2-)_2$], 2.5 [t, 2H, $-N-CH_2-CH_2-NH-CO-$], 3.1 [m, 6H, Lys$^{\omega}CH_2$ + Lys$^{\omega'}CH_2$ + Lys$^{\omega''}CH_2$], 3.3 [m, 2H, $-N-CH_2-CH_2-NH-CO$], 4.1 [m, 1H, LysC$^{\alpha}H$], 4.2−4.4 [m, 2H, LysC$^{\alpha'}H$ and LysC$^{\alpha''}H$], 5.0−5.1 [m, 3H, BOC−N*H*], 5.8 [m, 1 H, BOC−N*H*], 7.4−7.7 [m, 3H, N*H*−CO].

Step f. The compound prepared in step e (0.98 g, 0.78 mmol) was dissolved in 3 mL of dichloromethane/methanol (2:1, v/v), and 3 mL of methyl iodide was added to the solution. The reaction mixture was stirred at room temperature overnight, and the solvent was removed on a rotary evaporator. The residue upon column chromatographic purification with silica gel (60−120 mesh size) and 35% acetone in petroleum ether (v/v) as eluent afforded 0.66 g (61% yield) of *N*-2-[*N*′-(N^{α},N^{ϵ}-di-BOC-L-Lys-N^{ϵ}-BOC-L-Lys-N^{ϵ}-BOC-L-Lys)]aminoethyl-*N*,*N*-di-*n*-tetradecyl-*N*-methylammonium iodide as a colorless gummy solid (R_f = 0.19, 30% acetone in petroleum ether, v/v). ^{1}H NMR (300 MHz, CDCl$_3$): δ/ppm = 0.9 [t, 6H, $CH_3-(CH_2)_{11}-$], 1.2−1.4 [bs, 44H, $-(CH_2)_{11}-$], 1.3−1.6 [m, 12H, LysC$^{\gamma}H_2$ + LysC$^{\gamma'}H_2$ + LysC$^{\gamma''}H_2$ + LysC$^{\delta}H_2$ + LysC$^{\delta'}H_2$ + LysC$^{\delta''}H_2$], 1.4 [s, 36H, $-CO-O-C(CH_3)_3$], 1.7 [m, 6H, LysC$^{\beta}H_2$ + LysC$^{\beta'}H_2$ + LysC$^{\beta''}H_2$], 1.8−1.95 [m, 4H, $-N^+(-CH_2-CH_2-)_2$], 3.1 [m, 6H, Lys$^{\omega}CH_2$ + Lys$^{\omega'}CH_2$ + Lys$^{\omega''}CH_2$], 3.3 [s, 3H, $-N^+CH_3$], 3.4−3.5 [m, 4H, $-N^+(-CH_2-CH_2-)_2$], 3.7−3.8 [m, 4H, $-N^+-CH_2-CH_2-NH-CO-$], 4.1 [m, 1H, LysC$^{\alpha}H$], 4.3 [m, 2H, LysC$^{\alpha'}H$ and LysC$^{\alpha''}H$], 5.0−5.2 [bm, 3H, BOC−N*H*], 6.0 [m, 1H, BOC−N*H*], 7.6 [m, 1H, $-CH_2-CH_2-NH-CO-$], 7.8 [m, 1H, $-CO-CH-NH-CO-$], 7.9 [m, 1H, $-CO-CH-NH-CO-$].

Steps g and h. The quarternized intermediate prepared in step f (0.66 g, 0.47 mmol) was dissolved in dry DCM (3 mL), and TFA (3 mL) was added to the solution at 0 °C. The resulting solution was left stirred at room temperature overnight. Excess TFA was removed by flushing nitrogen to give the title compound as a trifluoroacetate salt. Repeated crystallization from diethyl ether/methanol (4:1, v/v) followed by chloride ion exchange chromatography (using Amberlyst A-26 chloride ion exchange resin) afforded 0.4 g (52.7% yield) the pure title compound DTML$_3$AC (R_f = 0.1, 30% methanol in dichlomethane, v/v). LSIMS (lipid **8**): *m*/*z* 852 [M$^+$] (calcd for $C_{49}H_{103}O_3N_8$, 60%).

DHML$_3$AC (Lipid 9). ^{1}H NMR (400 MHz, CDCl$_3$) of *N*-2-[*N*′-(N^{α},N^{ϵ}-di-BOC-L-Lys-N^{ϵ}-BOC-L-Lys-N^{ϵ}-BOC-L-Lys)]aminoethyl-*N*,*N*-di-*n*-hexadecyl-*N*-methylammonium iodide (**immediate precursor** of lipid **9**): δ/ppm = 0.9 [t, 6H, $CH_3-(CH_2)_{13}-$], 1.2−1.4 [bs, 52H, $-(CH_2)_{13}-$], 1.3−1.6 [m, 12H, LysC$^{\gamma}H_2$ + LysC$^{\gamma'}H_2$ + LysC$^{\gamma''}H_2$ + LysC$^{\delta}H_2$ + LysC$^{\delta'}H_2$ + LysC$^{\delta''}H_2$], 1.4 [s, 36H, $-CO-O-C(CH_3)_3$], 1.7 [m, 6H, LysC$^{\beta}H_2$ + LysC$^{\beta'}H_2$ + LysC$^{\beta''}H_2$], 1.8−1.95 [m, 4H, $-N^+(-CH_2-CH_2-)_2$], 3.1 [m, 6H, Lys$^{\omega}CH_2$ + Lys$^{\omega'}CH_2$ + Lys$^{\omega''}CH_2$], 3.3 [s, 3H, $-N^+CH_3$], 3.35−3.45 [m, 4H, $-N^+(-CH_2-CH_2-)_2$], 3.65−3.8 [m, 4H, $-N^+-CH_2-CH_2-NH-CO-$], 4.1 [m, 1H, LysC$^{\alpha}H$], 4.3 [m, 2H, LysC$^{\alpha'}H$ and LysC$^{\alpha''}H$], 5.0−5.2 [bm, 3H, BOC N*H*], 6.0 [m, 1H, BOC N*H*], 7.6 [m, 1H, $-CH_2-CH_2-NH-CO-$], 7.8 [m, 1H, $-CO-CH-NH-CO-$], 7.9 [m, 1H, $-CO-CH-NH-CO-$]. LSIMS: *m*/*z* 908 [M$^+$] (calcd for $C_{53}H_{111}O_3N_8$, 4^0 ammonium ion, 14%).

DOML$_3$AC (Lipid 10). ^{1}H NMR (200 MHz, CDCl$_3$) of *N*-2-[*N*′-(N^{α},N^{ϵ}-di-BOC-L-Lys-N^{ϵ}-BOC-L-Lys-N^{ϵ}-BOC-L-Lys)]aminoethyl-*N*,*N*-di-*n*-octadecyl-*N*-methylammonium iodide (immediate precursor of lipid **10**): δ/ppm = 0.9 [t, 6H, $CH_3-(CH_2)_{15}-$], 1.2−1.4 [bs, 44H, $-(CH_2)_{15}-$], 1.3−1.6 [m, 12H, LysC$^{\gamma}H_2$ + LysC$^{\gamma'}H_2$ + LysC$^{\gamma''}H_2$ + LysC$^{\delta}H_2$ + LysC$^{\delta'}H_2$ + LysC$^{\delta''}H_2$], 1.4 [s, 36H, $-CO-O-C(CH_3)_3$], 1.6−1.95 [m, 10H, LysC$^{\beta}H_2$ + LysC$^{\beta'}H_2$ + LysC$^{\beta''}H_2$ + $-N^+(-CH_2-CH_2-)_2$], 3.1 [m, 6H, Lys$^{\omega}CH_2$ + Lys$^{\omega'}CH_2$ + Lys$^{\omega''}CH_2$], 3.3 [s, 3H, $-N^+CH_3$], 3.4−3.5 [m, 4H, $-N^+(-CH_2-CH_2-)_2$], 3.7−3.8 [m, 4H, $-N^+-CH_2-CH_2-NH-CO-$], 4.1 [m, 1H, LysC$^{\alpha}H$], 4.3[m, 2H, LysC$^{\alpha'}H$ and LysC$^{\alpha''}H$], 5.0−5.2 [bm, 3H, BOC N*H*], 6.0 [m, 1H, BOC N*H*], 7.6−7.8 [m, 2H, $-CH_2-CH_2-NH-CO-$ + $-CO-CH-NH-CO-$], 7.95 [m, 1H, $-CO-CH-NH-CO-$]. LSIMS: *m*/*z* 964 [M$^+$] (calcd for $C_{57}H_{123}O_3N_8$, 4^0 ammonium ion, 12%).

Cell Culture. COS-1 (SV 40 transformed African green monkey kidney cells), CHO (Chinese hamster ovary), and

HepG2 (human hepatocarcinoma) cell lines were procured from the National Centre for Cell Sciences (NCCS), Pune, India. Cells were cultured at 37 °C in Dulbecco's modified Eagle's medium (DMEM) with 10% fetal bovine serum, 50 μg/mL penicillin, 50 μg/mL streptomycin, and 20 μg/mL kanamycin in a humidified atmosphere containing 5% CO_2.

Preparation of Liposomes. The cationic lipid and the colipid (Chol or DOPE) in 1:1 mole ratio were dissolved in a mixture of chloroform and methanol (3:1, v/v) in a glass vial. The solvent was removed with a thin flow of moisture-free nitrogen gas, and the dried lipid film was then kept under high vacuum for 8 h. An amount of 5 mL of sterile deionized water was added to the vacuum-dried lipid film, and the mixture was allowed to swell overnight. The vial was then vortexed for 2−3 min at room temperature and occasionally sonicated in a bath sonicator to produce multilamellar vesicles (MLVs). MLVs were then sonicated in an ice bath until clear using a Branson 450 sonifier at 100% duty cycle and 25 W output power. The resulting clear aqueous liposomes were used in forming lipoplexes.

Plasmid DNA. pCMV-SPORT-β-gal plasmids were a generous gift from Dr. Nalam Madhusudhana Rao (Centre for Cellular and Molecular Biology, Hyderabad, India) and were amplified in DH5α strain of *Escherichia coli*, isolated by alkaline lysis procedure, and finally purified by PEG-8000 precipitation as described previously.[35] The purity of plasmid was checked by A_{260}/A_{280} ratio (around 1.9) and 1% agarose gel electrophoresis.

Transfection of Cells. Cells were seeded at a density of 15 000 (for COS-1) and 20 000 cells (for CHO and HepG2) per well in a 96-well plate 18−24 h before the transfection. An amount of 0.3 μg of plasmid DNA was complexed with varying amounts of lipids (0.033−2.7 nmol for the monolysine series, 0.025−2.025 nmol for dilysine series, and 0.02−1.62 nmol for trilysine series) in plain DMEM medium (total volume made up to 100 μL) for 30 min. The charge ratios were varied from 0.1:1 to 9:1 over these ranges of the lipids. Immediately prior to transfection, cells plated in the 96-well plate were washed with PBS (2 × 100 μL) followed by the addition of lipoplexes. After 3 h of incubation, 100 μL of DMEM with 20% FBS was added to the cells. The medium was changed to 10% complete medium after 24 h, and the reporter gene activity was estimated after 48 h. The cells were washed twice with PBS (100 μL each) and lysed in 50 μL of lysis buffer [0.25 M Tris-HCl (pH 8.0) and 0.5% NP40]. Care was taken to ensure complete lysis. The β-galactosidase activity per well was estimated by adding 50 μL of 2X-substrate solution [1.33 mg/mL of ONPG, 0.2 M sodium phosphate (pH 7.3) and 2 mM magnesium chloride] to the lysate in a 96-well plate. Absorbance of the product *o*-nitrophenol at 405 nm was converted to β-galactosidase units by using a calibration curve constructed using pure commercial β-galactosidase enzyme. Each transfection experiment was repeated three times on three different days. The transfection values reported were average values from three replicate transfection plates assayed on three different days. The values of β-galactosidase units in replicate plates assayed on the same day varied by less than 20%. The day to day variation in transfection efficiency values for identically treated transfection plates was mostly within 2- to 3-fold and was dependent on the cell density and condition of the cells.

Toxicity Assay. Cytotoxicities of the lipids **1**−**10** were assessed by the 3-(4,5-dimethylthiazol-2-yl)-2,5-diphenyltetrazolium bromide (MTT) reduction assay as described earlier.[4] The cytotoxicity assay was performed in 96-well plates by maintaining the same ratio of number of cells to amount of cationic lipid, as used in the transfection experiments. MTT was added 3 h after addition of cationic lipid to the cells. Results were expressed as percent viability = {[A_{540}(treated cells) − background]/[A_{540}(untreated cells) − background]} × 100.

ζ Potential and Size Measurements. The sizes and the surface charges (ζ potentials) of liposomes and lipoplexes were measured by photon correlation spectroscopy and electrophoretic mobility on a Zeta sizer 3000HS_A (Malvern, U.K.). The sizes were measured in deionized water with a sample refractive index of 1.59 and a viscosity of 0.89. The system was calibrated by using a 200 ± 5 nm polystyrene polymer (Duke Scientific Corps., Palo Alto, CA). The diameters of liposomes and lipoplexes were calculated by using the automatic mode. The ζ potential was measured using the following parameters: viscosity, 0.89 cP; dielectric constant, 79; temperature, 25 °C; *F*(Ka), 1.50 (Smoluchowski); maximum voltage of the current, V. The system was calibrated by using the DTS0050 standard from Malvern. Measurements were done 10 times with the zero-field correction. The potentials were calculated by using the Smoluchowski approximation.

Gel Retardation Assay. DNA/lipid complexes were formed by mixing 5 μL of plasmid DNA (0.1 μg/μL in 10 mM Hepes buffer, pH 7.4) with varying amounts of cationic lipids so that the final lipid/DNA charge ratios were mainted at 0.1:1 to 9:1 in a total volume of 50 μL. Complexes were incubated for 30 min at room temperature, after which 15 μL of each lipoplex was loaded on a 1% agarose gel and electrophoresed (100 V, 2 h). The bands were visualized with ethidium bromide staining.

DNase 1 Sensitivity Assays. Briefly, in a typical assay, 1.5 nmol of DNA (500 ng) was complexed with lipid using the indicated lipid/DNA charge ratios (Figure 5B) in 10 mM Hepes buffer (pH 7.4) in a volume of 40 μL, and the mixture was incubated at room temperature for 30 min on a rotary shaker. Subsequently, the complexes were treated with DNase I (at a final concentration of 1 ng/1.5 nmol of DNA) in the presence of 10 mM $MgCl_2$ and incubated for 20 min at 37 °C. The reactions were then halted by adding EDTA (to a final concentration of 50 mM) and incubated at 60 °C for 10 min in a water bath. The aqueous layer was washed with 50 μL of phenol/chloroform mixture (1:1, v/v) and centrifuged at 10000*g* for 5 min. The aqueous supernatants were separated, loaded (15 μL) on a 1% agarose gel, and electrophoresed at 100 V for 2 h. The bands were visualized with ethidium bromide staining.

Acknowledgment. Financial support (to A.C.) received from the Department of Biotechnology, Government of India, New Delhi, is gratefully acknowledged. P.P.K. and V.V.K. acknowledge the Senior Research Fellowships received from the University Grant Commision and Council of Scientific and Industrial Research, Government of India, respectively.

Appendix

Abbreviations: Boc, *tert*-butyloxycarbonyl; Chol, cholesterol; DCC, dicyclohexylcarbodiimide; DCM, dichloromethane; DMAP, 4-(dimethylamino)pyridine; DMEM, Dulbecco's modified Eagle's medium; DMF, *N*,*N*-dimethylformamide; DOPE, 1,2-dioleoyl-*sn*-glycero-3-phosphoethanolamine; FBS, fetal bovine serum; HOSu, *N*-hydroxysuccinimide; DTMLAC, *N*,*N*-di-*n*-tetradecyl-*N*-methyl-*N*-2-[*N*′-(L-Lysyl)]aminoethylammonium chloride; DHMLAC, *N*,*N*-di-*n*-hexadecyl-*N*-methyl-*N*-2-[*N*′-(L-Lysyl)]aminoethylammonium chloride; DOMLAC, *N*,*N*-di-*n*-octadecyl-*N*-methyl-*N*-2-[*N*′-(L-Lysyl)]aminoethylammonium chloride; OOMLAC, *N*-*n*-octadecyl-*N*-oleyl-*N*-methyl-*N*-2-[*N*′-(L-Lysyl)]aminoethylammonium chloride; $DTML_2AC$, *N*,*N*-di-*n*-tetradecyl-*N*-methyl-*N*-2-[*N*′-(L-Lysyl)$_2$]aminoethylammonium chloride; $DHML_2AC$, *N*,*N*-di-*n*-hexadecyl-*N*-methyl-*N*-2-[*N*′-(L-Lysyl)$_2$]aminoethylammonium chloride; $DOML_2AC$, *N*,*N*-di-*n*-octadecyl-*N*-methyl-*N*-2-[*N*′-(L-Lysyl)$_2$]aminoethylammonium chloride; $DTML_3AC$, *N*,*N*-di-*n*-tetradecyl-*N*-methyl-*N*-2-[*N*′-(L-Lysyl)$_3$]aminoethylammonium chloride; $DHML_3AC$, *N*,*N*-di-*n*-hexadecyl-*N*-methyl-*N*-2-[*N*′-(L-Lysyl)$_3$]aminoethylammonium chloride; $DOML_3AC$, *N*,*N*-di-*n*-octadecyl-*N*-methyl-*N*-2-[*N*′-

(L-Lysyl)$_3$]aminoaminoethylammonium chloride; ONPG, *o*-nitrophenyl-*β*-D-galactopyranoside; PBS, phosphate-buffered saline; TFA, trifluoroacetic acid; Z, benzyloxycarbonyl.

Supporting Information Available: Reversed-phase HPLC chromatograms for all target lipids **1**−**10** in two mobile phases plus details of used HPLC parameters. This material is available free of charge via the Internet at http://pubs.acs.org.

References

(1) Vinod Kumar, V.; Singh, R. S.; Chaudhuri, A. Cationic Transfection Lipids in Gene Therapy: Successes, SetBacks, Challenges and Promises. *Curr. Med. Chem.* **2003**, *10*, 1297−1306 and references therein.

(2) Kumar, V. V.; Pichon, C.; Refregiers, M.; Guerin, B.; Midoux, P.; Chaudhuri, A. Single histidine residue in head-group region is sufficient to impart remarkable gene transfection properties to cationic lipids: evidence for histidine-mediated membrane fusion at acidic pH. *Gene Ther.* **2003**, *10*, 1206−1215.

(3) Heyes, J. A.; Duvaz, D. N.; Cooper, R. G.; Springer, C. J. Synthesis of Novel Cationic Lipids: Effect of Structural Modification on the Efficiency of Gene Transfer. *J. Med. Chem.* **2002**, *45*, 99−114.

(4) Singh, S. R.; Mukherjee, K.; Banerjee, R.; Chaudhuri, A.; Hait, S. K.; Moulik, S.; Ramadas, Y.; Vijayalakshmi, A.; Rao, N. M. Anchor-dependency for non-glycerol based cationic lipofectins: mixed bag of regular and anomalous transfection profiles. *Chem.—Eur. J.* **2002**, *8*, 900−909.

(5) McGregor, C.; Perrin, C.; Monck, M.; Camilleri, P.; Kirby, A. J. Rational approaches to the design of cationic gemini surfactants for gene delivery. *J. Am. Chem. Soc.* **2001**, *123*, 6215−6220.

(6) Banerjee, R.; Mahidhar, Y. V.; Chaudhuri, A.; Gopal, V.; Rao, N. M. Design, synthesis and transfection biology of novel cationic glycolipids for use in liposomal gene delivery. *J Med. Chem.* **2001**, *44*, 4176−4185.

(7) Pitard, B.; Oudrhiri, N.; Lambert, O.; Vivien, E.; Masson, C.; Wetzer, B.; Hauchecorne, M.; Scherman, D.; Rigaud, J. L.; Vigneron, J. P.; Lehn, J. M.; Lehn, P. Sterically stabilized BGTC-based lipoplexes: structural features and gene transfection into the mouse airways in vivo. *J. Gene Med.* **2001**, *3*, 478−487.

(8) Choi, J. S.; Lee, E. J.; Jang, H. S.; Park, J. S. New cationic liposomes for gene transfer into mammalian cells with high efficiency and low toxicity. *Bioconjugate Chem.* **2001**, *12*, 108−113.

(9) Guenin, E.; Herve, A. C.; Floch, V.; Loisel, S.; Yaounac, J.-J.; Clement, J. C.; Ferec, C.; Abbayes, H. D. Cationic phosphonolipids containing quaternary phosphonium and arsonium groups for DNA transfection with good efficiency and low cellular toxicity. *Angew. Chem., Int. Ed.* **2000**, *39*, 629−631.

(10) Floch, V.; Loisel, S.; Guenin, E.; Herve, A. C.; Clement, J. C.; Yaouanc, J. J.; Abbayes, H. D.; Ferec, C. Cation substitution in cationic phosphonolipids: a new concept to improve transfection activity and decrease cellular toxicity. *J. Med. Chem.* **2000**, *43*, 4617−4628.

(11) Fichert, T.; Regelin, A.; Massing, U. Synthesis and transfection properties of novel nontoxic monocationic lipids: variations of lipid anchor, spacer and headgroup structure. *Bioorg. Med. Chem. Lett.* **2000**, *10*, 787−791.

(12) Banerjee, R.; Das, P. K.; Srilakshmi, G. V.; Chaudhuri, A.; Rao, N. M. A novel series of non-glycerol based cationic transfection lipids for use in liposomal gene delivery. *J. Med. Chem.* **1999**, *42*, 4292−4299.

(13) Gerardo, B.; Catherine, D.; Virginie, E.; Marc, F.; Gabrielle, J.; Ravi, R.; Bruno, P.; Joel, C.; Pierre, W.; Bertrand, S.; Daniel, S. Synthesis, Activity, and Structure−Activity Relationship Studies of Novel Cationic Lipids for DNA Transfer. *J. Med. Chem.* **1998**, *41*, 224−235.

(14) Wang, J. K.; Guo, X.; Xu, Y.; Barron, L.; Szoka, F. C., Jr. Synthesis and Characterization of Long Chain Alkyl Acyl Carnitine Esters. Potentially Biodegradable Cationic Lipids for Use in Gene Delivery. *J. Med. Chem.* **1998**, *41*, 2207−2215.

(15) Miller, A. D. Cationic Liposomes in Gene Therapy. *Angew. Chem., Int. Ed.* **1998**, *37*, 1768−1785 and references therein.

(16) Gao, X.; Huang, L. Cationic liposome-mediated gene transfer. *Gene Ther.* **1995**, *2*, 710−722.

(17) Solodin, I.; Brown, C. S.; Bruno, M. S.; Chow, C. Y.; Jang, E. H.; et al. A novel series of amphiphilic imidazolinium compounds for in vitro and in vivo gene delivery. *Biochemistry* **1995**, *34*, 13537−13544.

(18) Brigham, K. L.; Meyrick, B.; Christman, B.; Magnuson, M.; King, G.; Berry, L. C., Jr. In vivo transfection of murine lungs with a functioning prokaryotic gene using a liposome vehicle. *Am. J. Med. Sci.* **1989**, *298*, 278−281.

(19) Logan, J. J.; Bebok, Z.; Walker, L. C.; Peng, S.; Felgner, P. L.; Siegal, G. P.; Frizzel, R. A.; Dong, J.; Howard, M.; Matalon, S.; Lindsey, J. R.; DuVall, M.; Sorseher, E. J. Cationic lipids for reporter gene and CFTR transfer to rat pulmonary epithelium. *Gene Ther.* **1995**, *2*, 38−49.

(20) Caplen, N. J.: Alton, E. W.; Middleton, P. G.; Dorin, J. R.; Stevenson, B. J.; Gao, X.; Durham, S. R.; Jeffrey, P. K.; Hodson, M. E.; Coutelle, C.; Huang, L.; Porteous, D. J.; Williamson, R.; Geddes, D. M. Liposome-mediated CFTR gene transfer to the nasal epithelium of patients with cystic fibrosis. *Nat. Med.* **1995**, *1*, 39−46.

(21) Bally, M. B.; Harvie, P.; Wong, F. M. P.; Kong, S.; Wasan, E. K.; Reimer, D. L. Biological barriers to cellular delivery of lipid-based DNA carriers. *Adv. Drug Delivery Rev.* **1999**, *38*, 291−315.

(22) Zabner, J.; Fasbender, Al, J.; Moninger, T.; Poellinger, K. A.; Welsh, M. J. Cellular and molecular barriers to gene transfer by a cationic lipid. *J. Biol. Chem.* **1995**, *270*, 18997−19007.

(23) Friend, D. S.; Papahadjopoulos, D.; Debs, R. J. Endocytosis and intracellular pocesses accompanying transfection mediated by cationic liposomes. *Biochim. Biophys. Acta* **1996**, *1278*, 41−50.

(24) Xu, Y.; Szoka, F. C., Jr. Mechanism of DNA release from cationic liposome/DNA complexes used in cell transfection. *Biochemistry* **1996**, *35*, 5616−5623.

(25) Eastman, S. J.; Siegel, C.; Tousignant, J.; Smith, A. E.; Cheng, S. H.; Scheule, R. K. Biophysical Characterization of cationic lipid:DNA complexes. *Biochim. Biophys. Acta* **1997**, *1325*, 41−62.

(26) Felgner, J. H.; Kumar, R.; Sridhar, C. N.; Wheeler, C. J.; Tsai, Y.-J.; Border, R.; Ramsey, P.; Martin, M.; Felgner, P. L. Enhanced gene delivery and mechanism studies with a novel series of cationic lipid formulations. *J. Biol. Chem.* **1994**, *269*, 2550−2561.

(27) Ghosh, Y. K.; Visweswariah, S. S.; Bhattacharya, S. Nature of linkage between the cationic headgroup and cholesterol skeleton controls gene transfection efficiency. *FEBS. Lett.* **2000**, *473*, 341−344.

(28) Wheeler, C. J.; Felgner, P. L.; Tsai, Y. J.; Marshall, J.; Sukhu, L.; Doh, S. G.; Hartikka, J.; Nietupski, J.; Manthorpe, M.; Nichols, M. A novel cationic lipid greatly enhances plasmid DNA delivery andexpression in mouse lung. *Proc. Natl. Acad. Sci. U.S.A.* **1996**, *93*, 11454−11459.

(29) Laxmi, A. A.; Vijayalakshmi, P.; Kaimal, T. N. B.; Chaudhuri, A.; Ramadas, Y.; Rao, N. M. Novel non-glycerol based cytofectins with lactic acid derived head groups. *Biochem. Biophys. Res. Commun.* **2001**, *289*, 1057−1062.

(30) Srilakshmi, G. V.; Sen, J.; Chaudhuri, A.; Ramdas, Y.; Rao, N. M. Anchor-dependent Lipofection with Non-Glycerol Based Cytofectins Containing Single 2-Hydroxyethyl Head Groups. *Biochim. Biophys. Acta* **2002**, *1559*, 87−95.

(31) Cameron, F. H.; Moghaddam, M. J.; Bender, V. J.; Whittaker, R. G.; Mott, M.; Lockette, T. J. A transfection compound based on a versatile Tris linkage. *Biochim. Biophys. Acta* **1999**, *1417*, 37−50.

(32) Puyal, C.; Milhaud, P.; Bienvenüe, A.; Phillipot, J. R. A new cationic liposome encapsulating genetic material: A potential delivery system for polynucleotides. *Eur. J. Biochem.* **1995**, *228*, 697−703.

(33) Kircheis, R.; Wagner, E. Polycation/DNA complexes for in vivo gene delivery. *Gene Ther. Regul.* **2000**, *1*, 95−114.

(34) Bodanszky, M.; Bodanszky, A. *The Practice of Peptide Synthesis*; Springer-Verlag: Berlin, Heidelberg, 1984; p 20.

(35) Sambrook, J.; Fritsch, E. F.; Maniatis, T. *Molecular Cloning: A Laboratory Manual*, 2nd ed.; Cold Springer Harbor Laboratory Press: Cold Spring Harbor, NY, 1989.

JM030541+